Flash photolysis of 4-diazoisochroman-3-one in aqueous solution. Hydration of the carbene produced by loss of nitrogen and ketonization of the enol hydration product

Y. Chiang, S. J. Eustace, E. A. Jefferson, A. J. Kresge,* V. V. Popik and R.-Q. Xie

Department of Chemistry, University of Toronto, Toronto, Ontario M5S 3H6, Canada

epoc ABSTRACT: Flash photolysis of 4-diazoisochroman-3-one in aqueous solution resulted in loss of nitrogen and transient production of the α-carbonylcarbene 3-ketoisochroman-4-ylidene, the hydration of which generated a short-lived species that was identified as the enol isomer of the lactone, 4-hydroxyisochroman-3-one. This assignment is supported by x-ray crystallographic determination of the structure of the final lactone product, by the shape of the rate profile for ketonization of the enol intermediate to the lactone, and by solvent isotope effects on, and the form of acid–base catalysis of, the ketonization reaction. Copyright © 2000 John Wiley & Sons, Ltd.
*Additional material for this paper is available from the epoc website at http://www.wiley.com/epoc*

KEYWORDS: 4-diazoisochroman-3-one; flash photolysis; carbene hydration; ketonization

INTRODUCTION

We discovered several years ago that flash photolysis of methyl phenyldiazoacetate, **1**, in aqueous solution produces methyl mandelate, **4**, through two short-lived intermediates, which we identified as phenylcarbomethoxycarbene, **2**, and the enol of methyl mandelate, **3**, Eqn. (1).[1]

This behavior stands in marked contrast to that of *S*-methyl phenyldiazothioacetate, **5**, which, under the same conditions, undergoes a photo-Wolff rearrangement and produces α-(methylthio)phenylacetic acid, **8**, through ketene, **6**, and enol, **7**, intermediates, Eqn. (2).[2]

This difference in behavior undoubtedly stems from the poor migratory aptitude of oxygen[3] and the strong ability of sulfur to promote neighboring group displacement.[4] These effects, however, might also be augmented by a stereochemical factor. Calculations indicate that methyl phenyldiazoacetate exits predominantly in the *s-trans* configuration of diazo and carbonyl groups shown in **1**,[5] but it is believed that the photo-Wolff rearrangement occurs more readily from the *s-cis* configuration, shown in **9**, where the leaving and migrating groups are *trans* to one another.[6] This suggests that 4-diazoisochroman-3-one, **10**, whose cyclic structure enforces an *s-cis* configuration, will have a stronger tendency to undergo
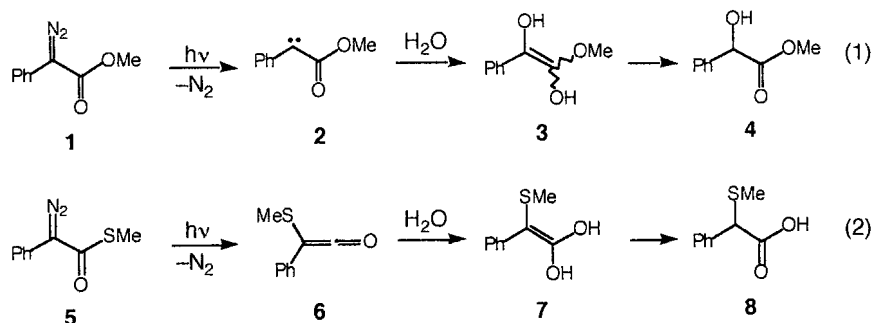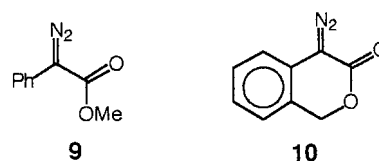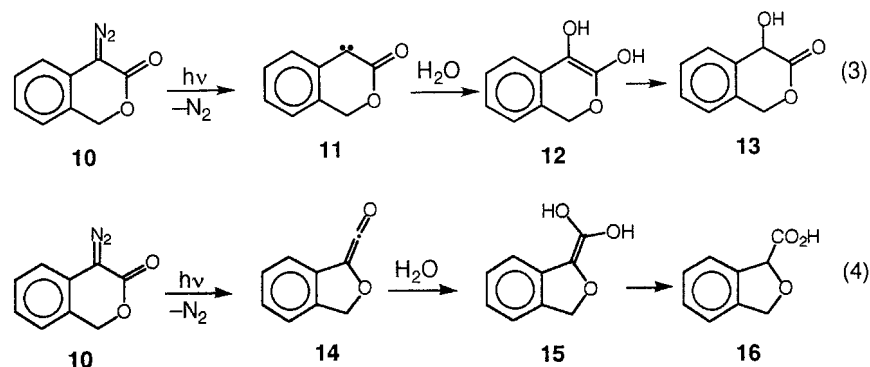
the Wolff rearrangement and that rearrangement might actually be the favored process in this case.

We have found, however, that this is not so: our investigation has shown that this cyclic substrate reacts by the same route as its acyclic analog and gives 4-hydroxyisochromane-3-one, **13**, as a final product through 3-ketoisochroman-4-ylidene, **11**, and 4-hydroxyisochroman-3-one enol, **12**, intermediates, Eqn. (3). This reaction route has nevertheless given us the opportunity of studying the chemistry of enol **12** and thereby contributing to the so far meager store of quantitative information about enols of carboxylic acid esters.

Some of this work has been published in preliminary form.[7]

EXPERIMENTAL

Materials. 4-Diazoisochroman-3-one was prepared from 3-isochromanone by diazo transfer with *p*-acetamido-benzenesulfonyl azide as the diazo source;[8] its spectral properties were consistent with literature values.[5a]

4-Hydroxyisochroman-3-one was obtained by photolysis of 4-diazoisochroman-3-one. A solution of the diazo compound (100 mg) in 3.0 ml of water containing 10% acetonitrile was irradiated for 30 min in a Rayonet apparatus operating at 300 nm. The solvent was then removed by rotary evaporation, giving a solid residue whose ^1H NMR spectrum contained only signals expected for 4-hydroxyisochroman-3-one.[5a]

All other materials were best-available commercial grades.

Kinetics. Rates of reaction were measured using conventional (flash lamp)[9] and laser ($\lambda = 248$ nm)[10] flash photolysis systems that have already been described. The temperature of all solutions upon which rate measurements were made was controlled at $2.50 \pm 0.05\,°C$. Two transient species were observed as a rise followed by a decay of absorbance in the region 315–340 nm. When the rates of reaction of these transients were sufficiently different, each reaction was

monitored in separate experiments and the data were analyzed by least-squares fitting of single exponential functions. When the rates were too similar to allow such separation, both reactions were monitored in the same experiment and the data were analyzed by least-squares fitting of either a single exponential plus linear function or a double exponential function.

RESULTS

Product determination

If flash photolysis of 4-diazoisochroman-3-one had led to a photo-Wolff rearrangement, the final product would have been 1,3-dihydrobenzo[*c*]furan-1-carboxylic acid, **16**, produced by hydration of 1,3-dihydrobenzo[*c*]furan-1-ylideneketene, **14**, and ketonization of the subsequent enol, **15**, as shown in Eqn. (4). This carboxylic acid is an isomer of the other possible flash photolysis product, 4-hydroxyisochroman-3-one [Eqn. (3), **13**], and these two substances cannot therefore be distinguished by high-resolution mass spectrometry. The NMR spectral properties of the two substances might also be expected to be similar. We consequently identified the reaction product by x-ray crystallography, which showed unequivocally that it is 2-hydroxyisochroman-3-one.[11] This is consistent with a recent report that 4-methoxyisochroman-3-one is the principal product formed by photolysis of 4-diazoisochromanone in methanol solution.[12]

This identification of 2-hydroxyisochroman-3-one as the reaction product establishes the sequence of reactions shown in Eqn. (3) as the process under observation. It also shows that the α-carbonylcarbene **11** and the enol **12** are the two successively formed transient species observed and that hydration of the carbene and ketonization of the enol are the two reactions that were monitored.

Kinetics: carbene hydration

Rates of hydration of 3-ketoisochroman-4-ylidene were measured in dilute aqueous perchloric acid and sodium hydroxide solutions. A range of concentrations was

**Table 1.** Summary of rate and equilibrium constants[a]

Process	Constant
(structure) $+ H_2O \xrightarrow{H^+}$ (structure)	$k_{H^+} = 2.30 \times 10^{10}\ \mathrm{l\,mol^{-1}\,s^{-1}}$
(structure) $+ H_2O \longrightarrow$ (structure)	$k_{uc} = 1.90 \times 10^{5}\ \mathrm{s^{-1}}$
(structure) $+ H_2O \xrightarrow{HO^-}$ (structure)	$k_{HO^-} = 1.09 \times 10^{10}\ \mathrm{l\,mol^{-1}\,s^{-1}}$
(structure) $\xrightarrow{H^+}$ (structure)	$k_{H^+} = 1.31 \times 10^{3}\ \mathrm{l\,mol^{-1}\,s^{-1}}$
(structure) $\xrightarrow{H^+}$ (structure)	$k'_{H^+} = 1.93 \times 10^{8}\ \mathrm{l\,mol^{-1}\,s^{-1}}$
(structure) $\xrightarrow{H_2O}$ (structure)	$k'_{0} = 3.65 \times 10^{4}\ \mathrm{l\,mol^{-1}\,s^{-1}}$
(structure) $\rightleftharpoons$ (structure) $+ H^+$	$Q_a^{E} = 2.05 \times 10^{-6}\ \mathrm{l\,mol^{-1}}\quad pQ_a^{E} = 5.69$

[a] Aqueous solution, 25 °C, ionic strength = 0.10 M.

employed for each kind of solution, and replicate measurements were made at each concentration; the ionic strength was maintained at 0.10 M. The data so obtained are summarized as supplementary Tables S1 and S2 at the epoc website http://www.wiley.com/epoc.

Rate measurements were also made in aqueous biphosphate ion, tris(hydroxymethyl)methylammonium ion, *tert*-butylphosphonate monoanion and ammonium ion buffers. Series of solutions of constant buffer ratio and constant ionic strength (0.10 M) but varying buffer concentration were used. These data are also summarized in supplementary Table S3 at the epoc website.

Observed first-order rate constants determined in buffer solutions increased linearly with increasing buffer concentration, and the data were therefore analyzed by least-squares fitting of the buffer dilution expression shown in Eqn. (5). The zero-buffer concentration intercepts, k_0, obtained in this way, together with the
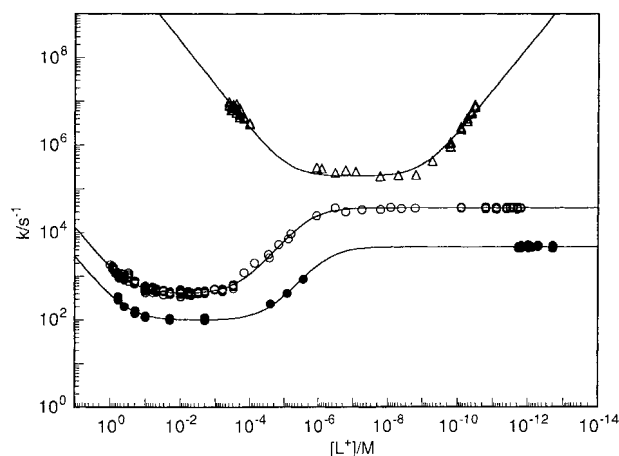
Figure 1. Rate profiles for the hydration of 3-ketoisochroman-4-ylidene in H_2O solution ($\triangle$) and the ketonization of the enol of 4-hydroxyisochroman-3-one in H_2O solution ($\bigcirc$) and D_2O solution ($\bullet$), all at 25 °C

rate constants measured in perchloric acid and sodium hydroxide solutions, are displayed as the uppermost rate profile in Fig. 1. Hydronium ion concentrations of the buffer solutions needed for this purpose were obtained by calculation, using literature values of the buffer acidity constants and activity coefficients recommended by Bates.[13]

$$k_{obs} = k_0 + k_{cat}[\text{buffer}] \qquad (5)$$

Kinetics: enol ketonization

Rates of ketonization of the enol of 4-hydroxyisochroman-3-one were measured in aqueous perchloric acid and sodium hydroxide solutions and in acetic acid, biphosphate ion and tris(hydroxymethyl)methylammonium ion buffers. Again, a range of concentrations was employed, replicate measurements were made and the ionic strength was maintained at 0.10 M, except in perchloric acid over the concentration range $[\text{HClO}_4] = 0.10$–1.0 M, where ionic strength $= [\text{HClO}_4]$. These data are summarized Tables S4–S6, at the epoc website

The measurements in buffers were made in series of solutions of constant buffer ratio but varying buffer concentration, and once again the observed first-order rate constants were found to increase linearly with increase in buffer concentration. The data were therefore also analyzed using Eqn. (5). The zero-buffer concentration intercepts so obtained, together with the rate constants measured in perchloric acid and sodium hydroxide solutions, were used to construct the middle rate profile shown in Fig. 1.

Some ketonization rate measurements were also made in D_2O solutions of perchloric acid, sodium hydroxide, and acetic acid buffers. These data are summarized in Tables S4–S6 at the epoc website and the rate profile that they provide is shown as the bottom curve in Fig. 1. This profile was constructed using literature values of the solvent isotope effects on the ionization of acetic acid[14] and the autoprotolysis of water.[15]

DISCUSSION

Carbene hydration

The rate profile for hydration of 3-ketoisochroman-4-ylidene shown in Fig. 1 is similar to the rate profiles for the analogous hydration of phenylcarboxycarbene[16] and phenylcarbomethoxycarbene.[1b] All three rate profiles show strong catalysis by hydronium and hydroxide ions in addition to an appreciable uncatalyzed reaction. Although the detailed mechanisms of these reactions are not known, the data may nevertheless be analyzed using the general rate law given in Eqn. (6). Least-squares fitting of this expression with the present

data gave $k_{H^+} = (2.30 \pm 0.10) \times 10^{10}\ \text{l mol}^{-1}\ \text{s}^{-1}$, $k_{uc} = (1.90 \pm 0.16) \times 10^5\ \text{s}^{-1}$ and $k_{HO^-} = (1.90 \pm 0.05) \times 10^{10}\ \text{l mol}^{-1}\ \text{s}^{-1}$.

$$k_{obs} = k_{H^+}[\text{H}^+] + k_{uc} + k_{HO^-}[\text{HO}^-] \qquad (6)$$

These rate constants are similar to the results obtained for phenylcarboxycarbene[16] and phenylcarbomethoxycarbene.[1b] The lifetimes of all three of these carbenes in the central uncatalyzed region of the rate profiles are 2–5 μs, which is considerably longer than the ca 1 ns lifetimes recently reported for other α-carbonylcarbenes.[17] Those short lifetimes, however, refer to reactions performed in non-polar organic solvents, unlike the wholly aqueous medium used in the present study. The short-lived carbenes also lacked a phenyl substituent next to the carbenic center. Such a phenyl substituent might be expected to stabilize the carbene, and microsecond lifetimes have in fact been reported for phenylcarbomethoxycarbene and 2-naphthylcarbomethoxycarbene in organic solvents.[18]

Strong catalysis of the hydration of 3-ketoisochroman-4-ylidene by buffer species was found for all of the buffers examined in the present study, consistent with the strong buffer catalysis found before for the hydration of phenylcarboxycarbene[16] and phenylcarbomethoxycarbene.[1b] In the present case, measurements at different buffer ratios were made for two of the buffers used, and the form of catalysis— general acid and/or general base— could consequently be determined. This was done with the aid of Eqn. (7):

$$k_{cat} = k_B + (k_{HA} - k_B)f_A \qquad (7)$$

where k_{cat} is the slope of the buffer dilution expression of Eqn. (5), k_B and k_{HA} are the general base and general acid catalytic coefficients and f_A is the fraction of buffer present in the acid form. Least-squares analysis gave $k_{HA} = (1.28 \pm 0.38) \times 10^8\ \text{l mol}^{-1}\ \text{s}^{-1}$ and $k_B = (3.57 \pm 0.63) \times 10^8\ \text{l mol}^{-1}\ \text{s}^{-1}$ for biphosphate ion buffers and $k_{HA} = (9.13 \pm 2.00) \times 10^7\ \text{l mol}^{-1}\ \text{s}^{-1}$ and $k_B = (2.28 \pm 0.02) \times 10^9\ \text{l mol}^{-1}\ \text{s}^{-1}$ for ammonium ion buffers.

Enol ketonization: rate profile

The rate profile for ketonization of the enol of 4-hydroxyisochroman-3-one shown in Fig. 1 is typical of rate profiles for ketonization of enols of carboxylic acids and esters.[1b,16,19] It is also consistent with the known mechanism for enol ketonization, which consists of rate-determining proton transfer from any available acid to the β-carbon atom of the enol or its enolate ion.[20] In aqueous solution at zero buffer concentration the available acids will be the hydronium ion (written here as H^+) and water

itself, and the reaction scheme may therefore be written as shown in Eqn. (8)
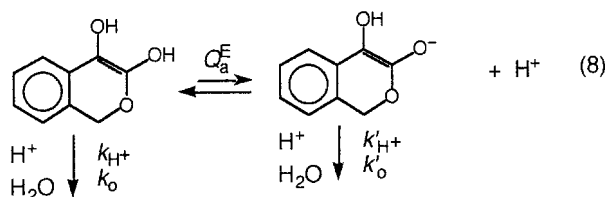

The acid-catalyzed region of this rate profile at high acidity then represents reaction of unionized enol through carbon protonation by H^+ (with rate constant k_{H^+}). This is followed by an uncatalyzed plateau extending from $[H^+] \approx 10^{-1}$ to 10^{-3} M, which could be caused either by carbon protonation of enol by H_2O (k_0) or by rapid equilibrium ionization of enol to the much more reactive[21,22] enolate ion (Q_a^E), followed by rate-determining carbon protonation of the enolate ion by H^+ (k'_{H^+}); this latter route produces H^+ in its first step and then consumes it in its second step, giving an overall process independent of $[H^+]$. The first of these two alternatives may be rejected because acid catalysis of the enol reaction does not set in until $[H^+] \approx 0.1$ M, which means that, if this uncatalyzed plateau were to be assigned to k_0, carbon protonation of the enol by H^+ and H_2O would be occurring at not very different rates; enol ketonization, however, obeys the Brønsted relation[21,22] and that requires proton transfer from acids of such widely different strengths as H^+ and H_2O to occur at different rates. The rate constant for reaction in this uncatalyzed plateau may therefore be written as $Q_a^E k'_{H^+}$.

At acidities below $[H^+] \approx 10^{-3}$ M, carbon protonation of the enolate ion by H_2O begins to compete with carbon protonation by H^+. The H^+ produced by equilibrium formation of enolate is then not consumed in the following step, and the rate of the overall reaction becomes inversely dependent on $[H^+]$ or directly
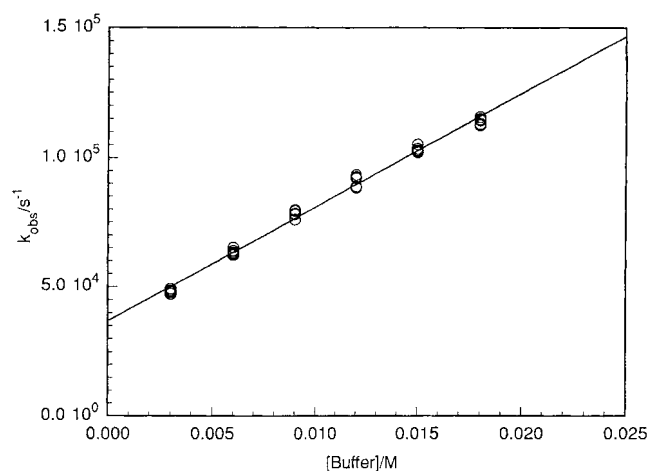
Figure 2. Buffer dilution plot for the ketonization of 4-hydroxyisochroman-3-one enol in aqueous biphosphate ion buffers at at 25 °C; $[H_2PO_4^-]/[HPO_4^=] = 2.00$
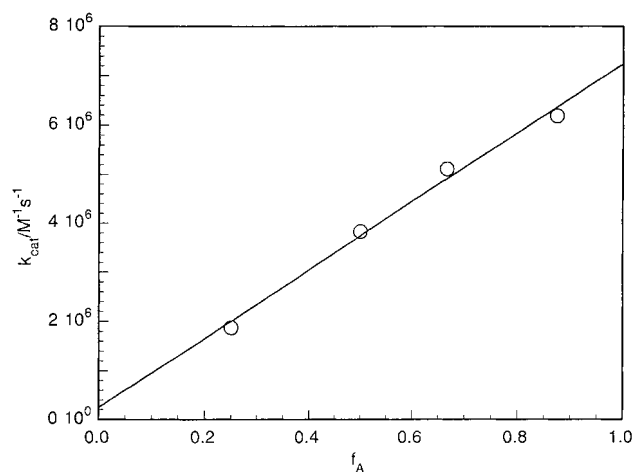
Figure 3. Separation of buffer catalysis into its general acid and general base components for the ketonization of 4-hydroxyisochroman-3-one enol in biphosphate ion buffers

dependent on $[HO^-]$. This appears as a rising profile segment extending down to $[H^+] \approx 10^{-6}$ M. Beyond that the position of the enol–enolate equilibrium shifts over to enolate, and the advantage of converting the less reactive enol to the more reactive enolate ion is lost; that produces the final horizontal plateau, representing simple carbon protonation of the enolate ion by H_2O.

The rate law that applies to this reaction scheme is shown in Eqn. 9, whose rate and equilibrium constants are defined by Eqn. (8). Least-squares fitting of this expression using the rate profile data obtained in H_2O solution gave $k_{H^+} = (1.31 \pm 0.03) \times 10^3$ $1\,mol^{-1}\,s^{-1}$, $k'_{H^+} = (1.93 \pm 0.99) \times 10^8\,1\,mol^{-1}$ s^{-1}, $k'_0 = (3.65 \pm 0.03) \times 10^4\,s^{-1}$, and $Q_a^E = (2.05 \pm 0.08) \times 10^{-6}\,1\,mol^{-1}$, $pQ_a^E = 5.69 \pm 0.02$. (This is a *concentration* acid dissociation constant, applicable at the ionic strength (0.10 M) at which it was determined.) Similar treatment of the data obtained in D_2O gave $k_{D^+} = (2.84 \pm 0.156) \times 10^2$ $1\,mol^{-1}\,s^{-1}$, $k'_{D^+} = (1.64 \pm 0.10) \times 10^8$ $1\,mol^{-1}\,s^{-1}$, $k'_0 = (4.69 \pm 0.05) \times 10^3\,s^{-1}$ and $Q_a^E = (6.03 \pm 0.33) \times 10^{-7}\,1\,mol^{-1}$, $pQ_a^E = 6.22 \pm 0.22$. (This is a *concentration* acid dissociation constant, applicable at the ionic strength (0.10 M) at which it was determined.)

$$k_{obs} = k_{H^+}[H^+] + (k'_{H^+}[H^+] + k'_0)\{Q_a^E/(Q_a^E + [H^+])\} \quad (9)$$

Enol ketonzation: isotope effects

These results give isotope effects that provide good support for the interpretation of the rate profile given above. The isotope effect on the portion of the rate profile assigned to carbon protonation of unionized enol by the hydronium ion, $k_{H^+}/k_{D^+} = 4.61 \pm 0.25$, is large. Such isotope effects contain an inverse ($k_H/k_D < 1$) secondary
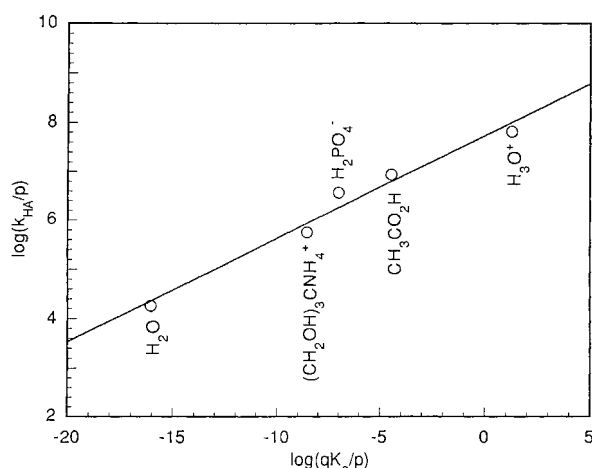
Figure 4. Brønsted plot for the ketonization of 4-hydro-xyisochroman-3-one enolate ion in aqueous solution at 25 °C

component that offsets the normal ($k_H/k_D > 1$) primary component, and the result obtained here is in fact a near maximum value.[22]

The isotope effect attributed to protonation of the enolate ion by hydronium ion, on the other hand, is much smaller: $k'_{H^+}/k'_{D^+} = 1.18 \pm 0.09$. This is consistent with the fact that the enolate ion reaction is a very fast, nearly diffusion-controlled process, and it should consequently have an early, reactant-like transition state in which the extent of proton transfer is still rather small.[23] Primary isotope effects are known to vary in magnitude with transition state structure, passing through a maximum value for symmetrical transition states in which the atom in flight is half-transferred, and falling off from this maximum for reactant-like and product-like transition states.[24] The primary component of the isotope effect on the enolate ion reaction can thus be expected to be small, and the secondary component will also be only poorly developed, producing an overall value close to unity. Similar small isotope effects have been observed before for the very rapid hydronium-ion protonation of iso-butyrophenone enolate ion ($k'_{H^+}/k'_{D^+} = 1.00 \pm 0.21$)[25] and of methyl mandelate enolate ion ($k'_{H^+}/k'_{D^+} = 1.14 \pm 0.13$).[1b]

The process attributed to carbon protonation of the enolate ion by water, on the other hand, is a much slower reaction, and its isotope effect is correspondingly larger: $(k'_0)_{H_2O}/(k'_0)_{D_2O} = 7.78 \pm 0.09$. This isotope effect also has a secondary component, this time in the normal direction, produced by solvation of the hydroxide ion formed by removal of a proton from H_2O,[26] and that will augment its value further. Similarly large isotope effects

have been found for the carbon protonation by water of isobutyrophenone enolate ion, $(k'_0)_{H_2O}/(k'_0)_{D_2O} = 7.48 \pm 0.23$,[25] mandelic acid enolate ion, $(k'_0)_{H_2O}/(k'_0)_{D_2O} = 6.90 \pm 0.54$,[16] and methyl mandelate enolate ion, $(k'_0)_{H_2O}/(k'_0)_{D_2O} = 7.74 \pm 0.40$.[1b]

The ionization of oxygen acids, such as the present enol, gives solvent isotope effects in the normal direction, and the value determined here, $(Q_a^E)_{H_2O}/(Q_a^E)_{D_2O} = 3.41 \pm 0.23$, is of the magnitude expected for an acid of the strength of the present enol.[27] Similar values have been obtained for the ionization of the enol of mandelic acid, $(Q_a^E)_{H_2O}/(Q_a^E)_{D_2O} = 4.47 \pm 0.55$,[16] and the enol of methyl mandelate, $(Q_a^E)_{H_2O}/(Q_a^E)_{D_2O} = 4.34 \pm 0.48$.[16]

Enol ketonization: buffer catalysis

The ketonization of enols, being a rate-determining proton transfer reaction, will show catalysis by acid–base buffer species, and this proved to be the case for the process assigned as ketonization of 4-hydroxyisochroman-3-one enol in all of the buffers examined here. An example of such catalysis is shown in the buffer dilution plot of Fig. 2.

Buffer catalytic coefficients, k_{cat}, were evaluated using Eqn. (5) and these were then separated into their general acid, k_{HA}, and general base, k_B, components with the aid of Eqn. (7) as is illustrated in Fig. 3. Least-squares analysis of the acetic acid buffer data showed significant general base catalysis, $k_B = (6.63 \pm 0.44) \times 10^5 \, \mathrm{l \, mol^{-1} \, s^{-1}}$, but produced no general acid catalysis, $k_{HA} = -(2.42 \pm 4.74) \times 10^4 \, \mathrm{l \, mol^{-1} \, s^{-1}}$, whereas the biphosphate ion and tris(hydroxymethyl)methylammonium ion data gave general acid catalysis, $k_{HA} = (7.23 \pm 0.23) \times 10^6 \, \mathrm{l \, mol^{-1} \, s^{-1}}$ and $k_{HA} = (1.69 \pm 0.15) \times 10^6 \, \mathrm{l \, mol^{-1} \, s^{-1}}$, respectively, but no general base catalysis, $k_B = (2.39 \pm 2.89) \times 10^5 \, \mathrm{l \, mol^{-1} \, s^{-1}}$ and $k_B = -(0.79 \pm 1.14) \times 10^5 \, \mathrm{l \, mol^{-1} \, s^{-1}}$. These results are consistent with the fact that the hydronium ion concentrations of the biphosphate ion and tris(hydroxymethyl)methylammonium ion buffers were less than the ionization constant of the enol, and enolate ion was consequently the principal substrate form present in these solutions. Ketonization therefore occurred by simple rate-determining carbon protonation of the enolate ion by the buffer acids, which of course would be a general-acid-catalyzed process. The hydronium ion concentrations of the acetic acid buffers, on the other hand, were greater than the enol ionization constant, and non-ionized enol was therefore the principal substrate form present in these solutions. The enolate ion, however, being much more reactive than the
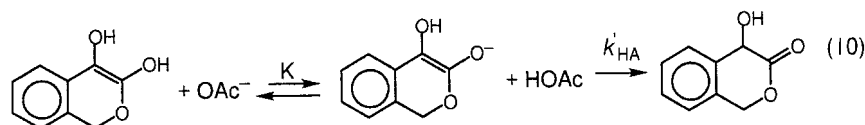
enol,[21] was still the species through which ketonization took place. The reaction therefore occurred through rapid equilibrium ionization of enol to enolate followed by rate-determining carbon protonation of the latter as shown in Eqn. (10), and that converted general acid catalysis of the rate-determining step into general base catalysis of the overall process.

The equilibrium constant of the first step in the reaction scheme of Eqn. (10) is equal to the ratio of acid ionization constants of the enol and acetic acid, $K = Q_a^E / Q_a^{HOAc}$, both of which are known. The general acid catalytic coefficient for carbon protonation of the enolate ion by acetic acid may therefore be evaluated from the relationship $k'_{HA} = k_B Q_a^{HOAc} / Q_a^E$ to give $k'_{HA} = (8.78 \pm 0.69) \times 10^6\,l\,mol^{-1}\,s^{-1}$.

General acid catalytic coefficients for the ketonization of enols obey the Brønsted relation[21] and, although the currently determined data refer to acids of fairly mixed charge type, they do give the reasonably good Brønsted plot shown in Fig. 4. The Brønsted exponent provided by this correlation, $\alpha = 0.21 \pm 0.02$, is low, which is consistent with the great speed of the reactions involved and their consequent early transition states.[23,28]

Buffer catalysis was also found for the ketonization of 4-hydroxyisochroman-3-one enol in acetic acid buffers in D_2O solution, and treatment of the data in a manner analogous to that used for acetic acid buffers in H_2O gave the general acid catalytic coefficient $k'_{DA} = (3.51 \pm 0.23) \times 10^6\,l\,mol^{-1}\,s^{-1}$. Combination of this result with its H_2O analog then produced the isotope effect $k'_{HA}/k'_{DA} = 2.50 \pm 0.25$. This is a modest effect, well below the maximum value expected for proton transfer to carbon from acetic acid, and that again is consistent with the rapidity of this reaction and its consequent early, unsymmetrical transition state.[23]

Acknowledgements

REFERENCES

1. (a) Chiang Y, Kresge AJ, Pruszynski P, Schepp NP, Wirz J. *Angew. Chem., Int. Ed. Engl.* 1991; **30**: 1366–1368; (b) Chiang Y, Kresge AJ, Schepp NP, Xie R-Q. *J. Org. Chem.* 2000; **65**: 1175–1180.
2. (a) Jones J Jr, Kresge AJ. *J. Org. Chem.* 1992; **57**: 6467–6469; (b) Chiang Y, Jefferson EA, Kresge AJ, Popik VV. *J. Am. Chem. Soc.* 1999; **121**: 11330–11335.
3. Meier H, Zeller K-P. *Angew. Chem. Int. Ed. Engl.* 1975; **14**: 32–43.
4. Hine J. *Physical Organic Chemistry* (2nd edn). McGraw-Hill: New York, 1962; 178–182.
5. (a) Jefferson EA, Kresge AJ, Paine SW. *Can. J. Chem.* 1996; **74**: 1369–1372; (b) Zhu Z, Bally T, Stracener LL, McMahon RJ. *J. Am. Chem. Soc.* 1999; **121**: 2863–2874.
6. Regitz M, Maas G. *Diazo Compounds Properties and Synthesis*. Academic Press: New York, 1986; 189–193.
7. Chiang Y, Jefferson EA, Kresge AJ, Popik VV, Xie Rl-Q. *J. Phys. Org. Chem.* 1998; **11**: 610–613.
8. Baum JS, Shook DA, Davies HML, Smith D. *Synth. Commun.* 1987; **17**: 1709–1716.
9. Chiang Y, Hojatti M, Keeffe JR, Kresge AJ, Schepp NP, Wirz J. *J. Am. Chem. Soc.* 1987; **109**: 4000–4009.
10. Andraos J, Chiang Y, Huang C-G, Kresge AJ, Scaiano JC. *J. Am. Chem. Soc.* 1993; **115**: 10605–10610.
11. Kresge AJ, Lough A, Popik VV. *Acta Crystallogr., Sect. C* 1999; **55**: IUC9900138.
12. Toscano JP. *Spectrum* 1999; **12**(2): 8–13.
13. Bates RG. *Determination of pH Theory and Practice*. Wiley: New York, 1973; 49.
14. Gary R, Bates RG, Robinson RG. *J. Phys. Chem.* 1965; **69**: 2750–2753; Gold V, Lowe BM. *J. Chem. Soc. A* 1968; 1923–1932.
15. Covington AK, Robinson RA, Bates RG. *J. Phys. Chem.* 1966; **70**: 3820–3824; Gold V, Lowe BM. *J. Chem. Soc. A* 1967; 936–943.
16. Chiang Y, Kresge AJ, Popik VV, Schepp NP. *J. Am. Chem. Soc.* 1997; **119**: 10203–10212.
17. Toscano JP, Platz MS, Nikolaev V, Popik VV. *J. Am. Chem. Soc.* 1994; **116**: 8146–8151; Toscano JP, Platz MS. *J. Am. Chem. Soc.* 1995; **117**: 4712–4713; Wang J-L, Toscano JP, Platz MS, Nikolaev V, Popik VV. *J. Am. Chem. Soc.* 1995; **117**: 5477–5483; Toscano JP, Platz MS, Nikolaev V, Cao Y, Zimmt BM. *J. Am. Chem. Soc.* 1996; **118**: 3527–3528.
18. Fujiwara Y, Tanimoto Y, Itoh M, Hirai K, Tomioka H. *J. Am. Chem. Soc.* 1987; **109**: 1942–1946; Wang Y, Yuzawa T, Hamaguchi H, Toscano JP. *J. Am. Chem. Soc.* 1999; **121**: 2875–2882; Wang J-L, Likhotvorik I, Platz MS. *J. Am. Chem. Soc.* 1999; **121**: 2883–2890.
19. Andraos J, Chiang Y, Kresge AJ, Pojarlieff IG, Schepp NP, Wirz J. *J. Am. Chem. Soc.* 1994; **116**: 73–81; Almstead J-IK, Urwyler B, Wirz J. *J. Am. Chem. Soc.* 1994; **116**: 954–960; Andaos J, Chiang Y, Kresge AJ, Popik VV. *J. Am. Chem. Soc.* 1997; **119**: 8417–8424.
20. Keeffe JR, Kresge AJ. In *The Chemistry of Enols*, Rappoport Z (ed). Wiley: New York, 1990; Chapt. 7.
21. (a) Pruszynski P, Chiang Y, Kresge AJ, Schepp NP, Walsh PA. *J. Phys. Chem.* 1986; **90**: 3760–3766. (b) Chiang Y, Kresge AJ, Santaballa JA, Wirz J. *J. Am. Chem. Soc.* 1988; **110**: 5506–5510.
22. Kresge AJ, Sagatys DS, Chen HL. *J. Am. Chem. Soc.* 1977; **99**: 7228–7233.
23. Hammond GS. *J. Am. Chem. Soc.* 1955; **77**: 334–338.
24. Melander L. *Isotope Effects on Reaction Rates*. Ronald Press: New York, 1960; 24–32; Westheimer F. *Chem. Rev.* 1961; **61**: 265–273; Bigeleisen J. *Pure Appl. Chem.* 1965; **8**: 217–223; Kresge AJ. In *Isotope Effects on Enzyme Catalyzed Reactions*, Cleland WW, O'Leary MH, Northrop DB (eds). University Park Press: Baltimore, MD, 1977; 37–63.
25. Chiang Y, Kresge AJ, Walsh PA. *Z. Naturforsch., Teil A* 1988; **44**: 406–412.
26. Gold V, Grist S. *J. Chem. Soc., Perkin Trans. 2* 1972; 89–95.
27. Laughton PM, Robertson RE. In *Solute–Solvent Interactions*, Coetzee JF, Ritchie CD (eds). Marcel Dekker: New York 1969; Chapt. 7.
28. Kresge AJ. In *Proton-Transfer Reactions*, Caldin EF, Gold V (eds). Chapman and Hall: London, 1975; Chapt. 7.